Brain Research 1848 (2025) 149329

Contents lists available at ScienceDirect

Brain Research

journal homepage: www.elsevier.com/locate/brainres

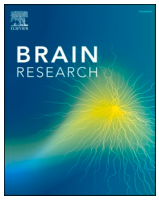

Research paper

Neurotranscriptomic and behavioral effects of ISRIB, and its therapeutic effects in the traumatic brain injury model in zebrafish

Nikita P. Ilyin [a,b], Anton D. Shevlyakov [c], Galina A. Boyko [a,b], Anastasia M. Moskalenko [c], Aleksey N. Ikrin [c], David S. Galstyan [a,b], Tatiana O. Kolesnikova [c], Nataliia V. Katolikova [b], Sergei A. Chekrygin [d], Lee Wei Lim [e,j], LongEn Yang [e,j], Murilo S. De Abreu [f,g], Konstantin B. Yenkoyan [h,i], Allan V. Kalueff [a,b,e,j,*], Konstantin A. Demin [a,b,*]

[a] Almazov National Medical Research Centre, St. Petersburg, Russia
[b] Institute of Translational Biomedicine, St. Petersburg State University, St. Petersburg, Russia
[c] Neurobiology Program, Sirius University of Science and Technology, Sochi, Russia
[d] Core Facility Center "Center Bio-Bank", Saint Petersburg University, St. Petersburg, Russia
[e] Department of Biosciences and Bioinformatics, School of Science, Xi'an Jiaotong-Liverpool University, Suzhou, China
[f] Graduate Program in Health Sciences, Federal University of Health Sciences of Porto Alegre, Porto Alegre, Brazil
[g] Western Caspian University, Baku, Azerbaijan
[h] Neuroscience Laboratory, Cobrain Center, M. Heratsi Yerevan State Medical University, Yerevan, Armenia
[i] Biochemistry Department, M. Heratsi Yerevan State Medical University, Yerevan, Armenia
[j] Suzhou Key Municipal Laboratory of Neurobiology and Cell Signaling, School of Science, Xi'an Jiaotong-Liverpool University, Suzhou, China

ARTICLE INFO

Keywords:
ISRIB
Integrated Stress Response
Traumatic brain injury
Transcriptome
Zebrafish
Behavioral deficits

ABSTRACT

Traumatic brain injury (TBI) is a global medical concern and has a lasting impact on brain activity with high risks of mortality. Current treatments are inadequate for repairing damaged brain cells or correcting cognitive and behavioral disabilities in TBI patients. Mounting evidence links TBI to the activation of the Integrated Stress Response (ISR) signaling in the brain. A novel small molecule, ISRIB, is an effective inhibitor of the ISR pathway, offering potential advantages for brain health. Here, we investigated how ISRIB affects brain transcriptome and behavior in zebrafish TBI model evoked by telencephalic brain injury. Overall, while TBI diminished memory and social behavior in zebrafish, administering ISRIB post-injury markedly reduced these behavioral deficits, and modulated brain gene expression, rescuing TBI-activated pathways related to inflammation and brain cell development. Collectively, this supports the role of brain ISR in TBI, and suggests potential utility of ISRIB for the treatment of TBI-related states.

1. Introduction

Traumatic brain injury (TBI), a damage of the brain tissue caused by an external force (Menon et al., 2010), represents a major medical and societal problem. With an estimated global prevalence of nearly 70 million people annually (James et al., 2019), TBI is accompanied by high risks of mortality and multiple disabilities (Finkelstein et al., 2006, Daneshvar et al., 2011, Coronado et al., 2012). Approximately 2 % of the global population has a TBI-related condition that commonly remains undiagnosed (Dewan et al., 2018). Furthermore, TBI pathogenesis extends beyond the *initial* neurotrauma, causing multiple *secondary* deficits, including motor dysfunctions, headache, loss of consciousness, cognitive impairment (e.g., attention and memory deficits), as well as frequently comorbid psychiatric conditions, especially depression and anxiety (Aldag et al., 2017; Delic et al., 2020; Sivanandam and Thakur, 2012; Walker and Tesco, 2013; Ding et al., 2016). TBI is recognized as one of the risk factors of multiple neurological disorders, such as Alzheimer's and Parkinson's diseases, as well as various forms of dementia and epilepsy (Delic et al., 2020; Graves et al., 1990; Guo et al., 2000; Johnson et al., 2010; Mortimer et al., 1985; Sivanandam and Thakur, 2012; Ding et al., 2016). Albeit severely debilitating, TBI currently has no available efficient and specific treatments that may restore the

* Corresponding authors at: Department of Biological Sciences, School of Science, Xi'an Jiaotong-Liverpool University, Suzhou, China (A.V. Kalueff). Institute of Translational Biomedicine SPBU, St. Petersburg, Russia (K.A. Demin).
E-mail addresses: avkalueff@gmail.com (A.V. Kalueff), deminkasci@gmail.com (K.A. Demin).

https://doi.org/10.1016/j.brainres.2024.149329
Received 11 June 2024; Received in revised form 5 October 2024; Accepted 9 November 2024
Available online 12 November 2024

induced neuronal damage, as well as behavioral and cognitive deficits.

Mounting evidence links TBI to hyperactive Integrated Stress Response (ISR) signaling in the brain (Petrov et al., 2001, Begum et al., 2014, Buffington et al., 2014, Scheper and Hoozemans 2015). ISR is a common regulatory pathway of eukaryotic cells that becomes activated in response to a wide range of severe cell stressors (Costa-Mattioli and Walter 2020, Di Domenico and Lanzillotta 2022). The downstream effects of ISR are primarily associated with the phosphorylation of eukaryotic translation initiation factor 2 alpha (eIF2α) by eIF2α kinases, such as PKR-like ER kinase (PERK), protein kinase double-stranded RNA-dependent (PKR), general control non-derepressible-2 (GCN2), and heme-regulated inhibitor (HRI), causing a global inhibition of protein translation and activation of some gene-specific mRNA translation (Donnelly et al., 2013, Ohno 2014, Costa-Mattioli and Walter 2020, Di Domenico and Lanzillotta 2022). Interestingly, in addition to its well-established role in the autophagy and protein homeostasis (B'chir et al., 2013, Wek 2018), ISR signaling is also implicated in memory via activating the transcription factor 4 (ATF4), a protein containing upstream open reading frames (uORFs) in their 5′UTR, whose mRNA translation is enhanced by ISR (Vattem and Wek 2004, Hinnebusch 2005, Jackson et al., 2010, Palam et al., 2011, Costa-Mattioli and Walter 2020). For example, hippocampal *Atf4* knockdown in mice impairs long-term spatial memory and behavioral flexibility (Pasini et al., 2015). Since the ISR system appears to play some role in the brain, it is therefore logical to assume that it may also contribute to TBI pathogenesis.

The ISR inhibitor, *trans*-N,N′-(Cyclohexane-1,4-diyl)bis(2-(4-chlorophenoxy)acetamide (ISRIB, Fig. 1), has been recently identified as a small experimental molecule reversing the effects of eIF2α phosphorylation (Sidrauski et al., 2013). In line with the role of ISR signaling in memory (and likely other CNS functions), ISRIB enhances spatial and fear-associated learning in mice (Sidrauski et al., 2013). Given the role of ISR role in neurodegeneration (Bond et al., 2020), this makes ISRIB a strong potential candidate to assess for its putative and clinically-relevant neuroactive effects. However, although ISRIB is currently extensively studied in rodents, supporting its beneficial effects in TBI (Chou et al., 2017, Krukowski et al., 2020, Frias et al., 2022, Zhou et al., 2023), the exact molecular mechanisms of its action in the brain, and the degree of their evolutionary conservation across taxa, remain poorly understood.

The zebrafish (*Danio rerio*) is a powerful model organism in neuroscience research that complements traditional rodent models and offers several unique experimental advantages. For example, their small body and brain size, rapid development, and high reproduction rates make zebrafish ideal for large-scale genetic, drug screening and neuroimaging studies, yet presenting relatively complex neuronal system (compared to other small model organisms) with high genetic and physiological homology to humans (Meshalkina et al., 2017, Wang and Cao 2021). These advantages have propelled zebrafish to the research frontiers in studying multiple neurodegenerative diseases and TBI (Bashirzade et al., 2022, Tikhonova et al., 2022). Zebrafish models are presently widely used for modeling neurotrauma, ranging from a needle puncture to laser ablation, with a detailed analysis of TBI impact on brain structure and function, as well as assessing temporal and spatial dynamics of molecular biomarkers of neurodegeneration and neuroregeneration (Chaoul et al., 2022, Tikhonova et al., 2022). Zebrafish also exhibit remarkable neuroregenerative abilities, allowing for restoration of multiple brain regions (Wang and Cao 2021), which also makes them a powerful model to probe molecular and cellular processes underlying neural restoration (Chaoul et al., 2022, Tikhonova et al., 2022). Capitalizing on this powerful in vivo system, the present study examined the effects of ISRIB on behavioral and neurotranscriptomic brain responses in vivo in both control and TBI-exposed adult zebrafish.

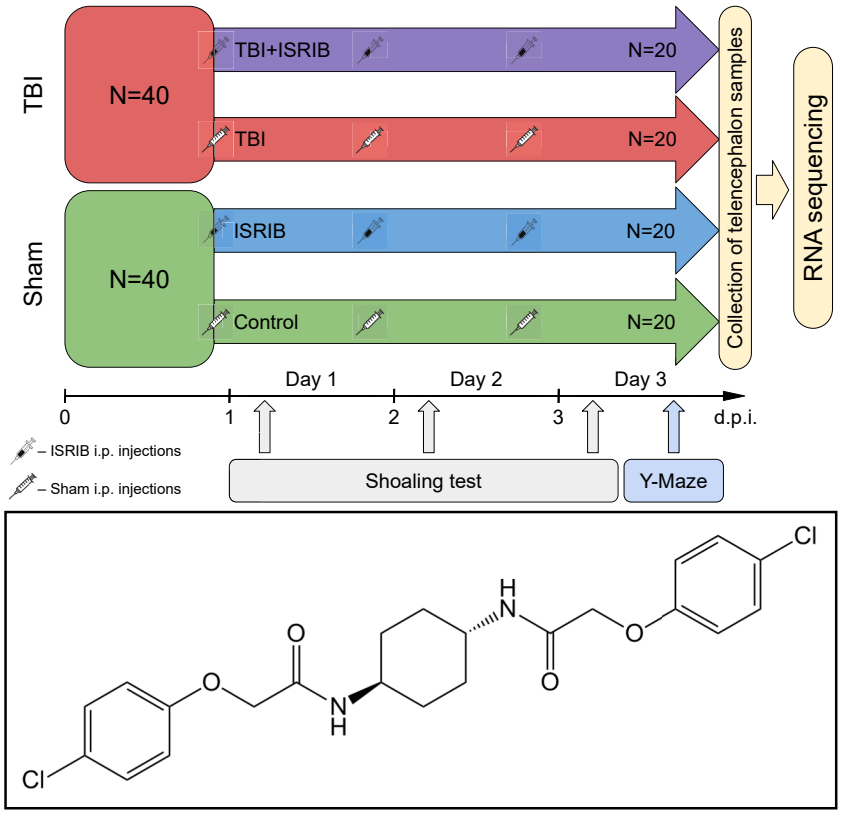

Fig. 1. A brief outline of the study experimental design and its timeline (the x-axis). TBI – traumatic brain injury, d.p.i. – days post-injury. Inset: chemical formula of ISRIB, the Integrated Stress Response (ISR) inhibitor. Syringe images denote timing of intraperitoneal (i.p.) injections of ISRIB or vehicle solutions to adult zebrafish.

2. Materials and methods

2.1. Animals and housing

The study utilized 80 adult (3–5 months old, ~1:1 male:female ratio) wild-type short-fin zebrafish obtained from a commercial vendor (Axolotl, LLC, St. Petersburg, Russia). The animals were kept in the Aquatic Facility of the Almazov National Medical Research Center (St. Petersburg, Russia) in accordance with standard zebrafish laboratory conditions (Westerfield 2007) in a ZebTec Active Blue Stand water distribution and purification system (Tecniplast, West Chester, USA), with lighting provided by ceiling-mounted neon light bulbs. The fish were housed in groups of 15 per 3-L holding tanks, with water temperature automatically maintained at 27 ± 0.5 °C, and the pH value at 7.4. The lighting intensity was 950–960 lx (as assessed by AE0903 luminometer, Open Science, Moscow, Russia), with a light/dark cycle of 14/10 h. The wild-type outbred short-fin zebrafish strain was used in the present study based on the population validity considerations for the CNS pathogenesis model. Specifically, while inbred zebrafish strains are more reliable for neurogenetic studies, modeling CNS pathologies involves recapitulating "real" human diseases in genetically heterogeneous populations. Thus, the use of outbred zebrafish is a more population-based and translationally relevant approach (Demin et al., 2019), consistent with the objectives of the present study.

Prior to the experiments, all animals underwent a 2-week acclimation to animal facility, were experimentally naive prior to this study, belonged to the same population and were randomly assigned to experimental groups using an online random number generator. All animals tested were included in the final analyses, with no outlier removal (unless specified otherwise for the Y-maze test). Every experiment proceeded as planned, and all analyses and endpoints were included without any omissions. The study experimental design and its description here, as well as data analysis and representation, adhered to the ARRIVE (Animal Research: Reporting of In Vivo Experiments) guidelines for reporting animal research, EU Directive 2010/63/EU for animal experiments, and the PREPARE (Planning Research and Experimental Procedures on Animals: Recommendations for Excellence) guidelines for planning animal research and testing.

2.2. Experimental design

The study experimental design is briefly outlined in Fig. 1. A total of 80 fish (1:1 male:female ratio) were randomly divided (using a random number online generator) into two equal cohorts: 40 fish subjected to TBI and 40 fish receiving sham injury (see further). Both cohorts were further randomly divided into two groups receiving intraperitoneal (i.p.) injections of ISRIB (control + ISRIB and TBI + ISRIB groups) or vehicle solution (control + vehicle and TBI + vehicle groups, n = 20 each). Each fish received a total of three injections with a one-day interval, as shown in Fig. 1. Behavioral testing was conducted over the next three days (experimental Days 1–3). The sample was determined based on the power analysis, similar to our previous studies (Demin et al., 2020), using the 4-group ANOVA model with type I error probability of 0.05 and power 0.80, yielding n = 19 animals per group for a large (f = 0.4) effect size.

2.3. Telencephalon stab wound injury (TBI model)

The stab wound injury was performed at 12:00–14:00 pm on the telencephalon of adult zebrafish, as described previously (Schmidt et al., 2014). Briefly, each zebrafish was anesthetized by immersion in a 170 mg/L phosphate-buffered tricaine (Sigma Aldrich, St. Louis, USA) until complete immobilization and then securely positioned on a tricaine-soaked sponge, to provide full access to the head area. The one-stab unilateral injury was induced by inserting an insulin needle (27 g) through the skull into the right hemisphere of the telencephalon (1.5–2 mm deep) under a dissection microscope. Immediately after the TBI procedure, the fish were placed into a holding tank for recovery. The procedure had 100 % survival rate in the present study, was performed consistently by the same highly trained experimenter, and the injury location was validated in 20 separate fish not included in behavioral testing (see Supplementary Fig. S1 for representative cryosection slides). Control + vehicle and control + ISRIB fish groups received a sham injury involving all procedures except for the skull/brain-penetrating needle insertion.

2.4. ISRIB intraperitoneal injections

The drug stock solution was prepared by dissolving 1 mg of ISRIB (RedPill, Moscow, Russia) in 0.5 ml of an organic solvent dimethyl sulfoxide (DMSO; Tula Pharmaceutical Factory, Tula, Russia). The solution was gently heated for several minutes until it became clear, and then 0.5 ml of polyethylene glycol 400 (PEG-400, Nizhnekamskneftekhim Ltd., Nizhnekamsk, Russia) was added to decrease DMSO concentration and increase tolerability. After vortexing for 2 min, the mix was stored at 4 °C and subsequently used for i.p. injections. The vehicle solution consisted of a drug-free 50:50 % (vol/vol) DMSO/PEG-400 mixture. The drug dosage was derived and extrapolated from rodent studies, where i.p. administration of 2.5 mg/kg ISRIB mitigates TBI-induced behavioral changes (Chou et al., 2017, Krukowski et al., 2020). The 1-μl injection volume was calculated based on our pilot studies and the average mass of experimental fish (approximately 0.383 g), delivered using the i.p. injection protocol described previously (Kinkel et al., 2010). For this, the fish were first anesthetized in cold water (12 °C) and then positioned on a sponge soaked in cold water with abdominal side up. The injection site was identified as the midline between the pelvic fins, posterior to the pelvic girdle (Kinkel et al., 2010). ISRIB injections were administered at 17:00–18:00 pm each day, using an automatic pipette connected to a 32-gauge injection needle. Fish of the control + vehicle and TBI + vehicle groups were similarly injected i.p. with an equal volume of drug-free vehicle solution.

2.5. Behavioral testing

Behavioral testing was performed between 10.00 am and 15.00 pm by highly trained experimenters on Days 1, 2 and 3 post-injury (Fig. 1) prior to i.p. injections and following a 1-h acclimation of fish to the testing room environment. The shoaling test is a widely used and robust behavioral assay assessing social and anxiety-like behaviors in zebrafish (Engeszer et al., 2007, Green et al., 2012, Pham et al., 2012). It involves placing a group of zebrafish in a tank and observing their tendency to group together, forming a shoal that is assessed using automated video-tracking software. The test was performed on Days 1–3 post-injury (Fig. 1) prior to i.p. injections. Each experimental group (n = 20) was placed into a rectangular tank (10 fish per group) and allowed to freely explore. Behavior was recorded for 15 min using a SJ4000 action camera (SJCAM, Ltd., Shenzhen, China) at 30 frames/s and analyzed offline using Noldus Ethovision XT15 software (Noldus IT, Wageningen, Netherlands), assessing average inter-fish distance and average velocity of zebrafish, based on object/body center point. The inter-fish distance was calculated as the distance between each fish tested and all other fish in the tank, resulting in 9 distances per fish tested (total 90 distances per group for 2 tanks of 10 fish each).

The free-movement pattern (FMP) Y-maze is commonly used to analyze working memory and behavioral flexibility in zebrafish and other laboratory animals (Cleal et al., 2021a,b). The test was performed following a protocol described previously (Cleal et al., 2021a, Cleal et al., 2021b, Fontana et al., 2021, Cleal et al., 2022), with minor modifications. The fish were introduced individually into white acrylic Y-shaped tanks filled with water. Each tank comprised three identical arms (50 length, 20 width, 140 height, mm) positioned at 120° angles to one another. Each fish was allowed to freely explore the maze for 15

min, recording right (R) or left (L) turns by top-mounted SJCAM SJ4000 action cameras. The videos were later analyzed offline using the Noldus Ethovision software, assessing fish entries into, and exit from, each arm of the maze. Data were expressed as a sequence of symbols, L or R. Two zebrafish (1 TBI + vehicle and 1 TBI + ISRIB) made < 100 turns per 15-min trial and were excluded from further analysis. The sequences generated for each fish were transformed into a frequency distribution of 16 overlapping tetragrams of alternative choices (LLLL, LLLR, LLRL, LLRR, LRLL, LRLR, LRRL, LRRR, RLLL, RLLR, RLRL, RLRR, RRLL, RRLR, RRRL, RRRR). The frequencies of tetragrams were normalized to the total number of turns and expressed as %, generating the percentages of alternations (tetragrams RLRL + LRLR) and repetitions (RRRR + LLLL).

2.6. Statistical analyses of behavioral data

Statistical analyses of behavioral data were performed using the R programming language (version 4.3.2). To examine dynamic behavioral changes in the shoaling test, we employed the Generalized Linear Models (GLM) approach, with factors 'Day' and 'Group' and their interaction as predictors. To determine the most suitable model for each behavioral endpoint, we fitted several models with different distributions and link functions, selecting the one with the lowest Akaike information criterion (AIC) value. For average (mean) velocity, the Gaussian distribution (identity link) was chosen, while the Gamma distribution (inverse link) was selected for average inter-fish distance. The significance of each predictor in the fitted models was assessed using the type II Wald chi-squared test (R package *car*, function 'Anova'). Pairwise comparisons between groups on each testing day were conducted using the 'emmeans' function (from the *emmeans* package), with Sidak adjustment for multiple comparisons. Results from the FMP Y-maze test were analyzed using the Kruskal-Wallis (KW) test, followed by Dunn's post-hoc test for pairwise comparisons for significant KW data.

2.7. RNA-sequencing and differential gene expression analyses

The collection of whole (both hemispheres) telencephalon samples was performed 3–5 h after the final behavioral test. The fish from all 4 groups (n = 9 per group) were euthanized by immersion in ice-cold water, and their telencephalon samples were extracted under the dissection microscope and frozen immediately at −80 °C for further analyses. RNA isolation was performed using the ExtractRNA reagent (Evrogen Lab LTD, Moscow, Russia) following the standard protocol for TriZol-mediated extraction. The RNA quality was verified by capillary electrophoresis using the QIAxcel Advanced program (QIAGEN, Hilden, Germany), excluding 8 specimens (distributed rather equally 2–3 per group) for low RNA quality. Total RNA was used for isolation of poly(A)-fraction using NEBNext® Poly(A) mRNA Magnetic Isolation Module (New England Biolabs Inc., Ipswich, UK) according to the manufacturer recommendations. RNA was next quantified on Quntus fluorometer (Promega Inc., Madison, USA) and used for library preparation using NEBNext® UltraTM Directional RNA Library PrepKit for Illumina® with NEBNext® Multiplex Oligos for Illumina® according to the manufacturer recommendations. The quality of libraries was confirmed by capillary electrophoresis using the QIAxcel Advanced program (QIAGEN), excluding 1 specimen due to insufficient quality. Pair-end sequencing was performed using Illumina HiSeq2500 (Illumina, Inc., San Diego, USA) with a read length of 110 bp (resulting in n = 5–8). The sequencing data is available from BioProject repository accession number PRJNA1111146 (https://www.ncbi.nlm.nih.gov/bioproject/1111146).

The row reads were processed by the Trimmomatic software v0.39 to remove adapters and cut low quality sequences (Bolger et al., 2014). The purified reads were mapped to the zebrafish GRCz11 reference transcriptome and quantified by Salmon pseudoalignment software v1.10.0 (Patro et al., 2015). Salmon was chosen as a tool based on a streaming variational Bayes (VB) inference algorithm, which is preferable for quantification reads of organisms containing many paralogues and pseudogenes, such as zebrafish, and helps avoid errors associated with false mapping of reads on a paralogical gene. The R software (Team, 2016) with the Bioconductor tximport package v1.28.0 (Huber et al., 2015, Soneson et al., 2015) was used to import transcript abundance (Team, 2016). The differential expression (DE) analysis was performed with DESeq2 Bioconductor package v1.40.2 (Love et al., 2014), chosen here as an effective tool for experiments containing 12 or fewer samples per condition, similarly to (Demin et al., 2020). A total of 25,859 genes were submitted for analysis and, after the DESeq2 matrix was created, all genes with <10 counts were filtered out, keeping a total of 18,755 remaining genes. The Negative Binomial (Gamma-Poisson) distribution generalized linear models and Wald statistics with counts normalization on size factor of library were used for analysis by DESeq function. The p-values were next adjusted using the Benjamini-Hochberg correction. P-value and false discovery rate (FDR) were set at 0.05. Genes were considered to be DE at $|\log2FoldChange| > 1$. A two-factor model was used for differential expression analysis. For gene DE analysis using DESeq2, three predictors were built in the negative binomial generalized linear model corresponding to factors: TBI (yes/no), ISRIB (yes/no) and TBI x ISRIB interaction. The factors were extracted from all 4 experimental groups utilized in the study: control + vehicle (TBI-ISRIB-), TBI + vehicle (TBI + ISRIB-), control + ISRIB (TBI-ISRIB +) and TBI + ISRIB (TBI + ISRIB +). The Principal Component Analysis (PCA) of the regularized log (rlog)-transformed data counts (Love et al., 2014) of 1000 the most differentially expressed genes based on their respective log2-fold change obtained in DESeq 2 analysis were used to estimate a general difference between groups (Supplementary Fig. S1). PCA was created by the plotPCA function from the DESeq2 package and visualized by the ggplot2 package v3.5.0 (Wickham et al., 2016). The corresponding analysis code and some intermediate data are available online at the Github repository (https://github.com/FLinT3/Transcriptomic-analysis-of-ISRIB-action-on-danio-rerio-brain-in-TBI-condition).

2.8. Gene set enrichment analyses (GSEA)

The Gene Set Enrichment Analysis (GSEA) is widely used to study pathways enrichment, allowing for a better detection of biologically relevant changes in gene expression data (Subramanian et al., 2005). GSEA was performed using Proteins with Values/Ranks − Functional Enrichment Analysis available in the STRING database (https://www.string-db.org) for Wald statistic values (log2-fold change divided by standard error) obtained following DESeq2 analysis. This analysis relies on Kolmogorov–Smirnov testing to detect significant pathways, followed by Aggregate Fold-Change testing where computationally feasible, evaluating the pathways for a skewed distribution on either end of the Wald statistic input, thus additionally reporting pathways that are simultaneously enriched on both ends of the input (but not the medium ranks, that were not significant in our Wald statistic values). Briefly, genes were ranked by a predefined statistic (log2 Fold Change/log2 Fold Change standard error), and an enrichment score (ES) was calculated by increasing or decreasing the score based on whether each gene belonged to the target gene set. The maximum ES was recorded as the final score. To assess significance, gene labels were shuffled 10,000 times, and ES values were recalculated to generate a null distribution. The nominal p-value was calculated by comparing the actual ES to the randomized ES values. The normalized enrichment score (NES) and false discovery rate (FDR) were also computed to account for multiple testing. The present study analyzed enrichment of the Gene Ontology (GO) Biological Process, GO Molecular Function, Kyoto Encyclopedia of Genes and Genomes (KEGG), and Zebrafish Phenotype Ontology (Monarch) pathways. REVIGO (https://www.revigo.irb.hr) online platform (Supek et al., 2011) was used to further group the related GO pathways into parent categories. Pathways with a false discovery rate < 0.01 were considered statistically significant.

To further investigate the association of factors with the influence of ATF4 on gene expression profiles across different experimental conditions, we conducted another customized GSEA, using only a gene set of putative ATF4 target genes. The list of putative ATF4 target genes was obtained from the recent review article, which compiled the existent ChiP and chromatin immunoprecipitation data in mammalian species (Neill and Masson 2023). Next, zebrafish orthologues of those genes were acquired using g:Profiler web-resource (https://biit.cs.ut.ee/gprofiler/orth). The custom GSEA was performed using the GSEA function (the R package 'clusterProfiler'), and the results were visualized using the functions gseaplot2 (R package 'enrichplot') and pheatmap (R package 'pheatmap'). P values < 0.001 were considered statistically significant in these analyses.

2.9. Weighted correlation network analysis (WGCNA)

The co-expression networks were built using weighted gene co-expression network analysis (WGCNA) (Langfelder and Horvath 2008). To construct a global weighted network, the (rlog)-transformed gene counts were used (Love et al., 2014). The absolute values of Pearson's correlation coefficients were calculated for all gene pairs and the resulting values were transformed using a β-power ($\beta = 12$) to ensure that the final correlation matrices followed an approximate scale-free topology. The WGCNA dynamic tree-cut algorithm was used to detect network modules (minimum module size = 30; cut tree height = 0.99; deep-split = 2, merge module height = 0.25). The module correlation was calculated only for two factors (TBI and ISRIB injection), without considering their interaction. The module genes with the most significant correlation between the factors were later used to assess over-representation for functional annotation of the clusters and in order to identify pathways that characterize the main differences between the groups using another GSEA approach. The ClusterProfiler software v4.8.3 was used for the GO Biological Process, GO Molecular Function, Go Cellular Component and KEGG pathways enrichment analysis (Yu et al., 2012), and the enrichment results were visualized using the Enrichplot package v1.20.3 (Wu et al., 2021). Additionally, we also assessed module-module relationships using Spearman correlation for the expression of modules found using WGCNA (Supplementary Fig. S3).

3. Results

3.1. Shoaling test

The shoaling test results revealed significant effects for Group and Day factor as well as their interaction for both the average velocity of individual fish and average inter-fish distance (Table 1; $p < 0.05$, analysis of deviance using Chi-Squared tests for GLM fits). To characterize behavioral dynamics in this test in detail, we performed pairwise within-day comparisons using the 'emmeans' contrasts assessment. TBI + vehicle decreased the mean velocity of zebrafish, and this effect persisted across all three testing days ($p < 0.001$ vs. control + vehicle group, Fig. 2). ISRIB i.p. injections notably improved locomotor activity of the TBI + ISRIB fish group on Day 1, reaching levels seen in control + vehicle fish on Days 2 and 3 of testing (Fig. 2). At the same time, ISRIB administered to healthy fish induced hypolocomotion on Days 2 and 3 ($p < 0.001$ vs. control + vehicle group, Fig. 2). TBI + vehicle markedly affected shoaling behavior of zebrafish (Fig. 2), reducing average inter-fish distance on Days 1–2 and increasing it on Day 3 ($p < 0.001$ vs. control + vehicle). In contrast, ISRIB treatment normalized this parameter on Days 2–3 ($p < 0.001$) in the TBI + vehicle group, whereas its injections alone significantly increased average inter-fish distance on Day 1 ($p < 0.01$ vs. control + vehicle group), but not on Days 2–3. No other overt motor deficits were observed in the any of the groups tested here (data not shown).

Table 1
Summary of significant effects on zebrafish behavior in the shoaling test determined by the Wald Chi-Squared tests (ANOVA Type II) for generalized linear models with factors Group, Day and their interaction as predictors.

Factor	χ2 chi square statistic	Df degree of freedom	p-value
Velocity, cm/s (Gaussian distribution, identity link)			
Group	599.448	3	<0.001
Day	101.033	2	<0.001
Group x Day	120.392	6	<0.001
Inter-fish distance, cm (Gamma distribution, inverse link)			
Group	42.469	3	<0.001
Day	85.957	2	<0.001
Group x Day	413.384	6	<0.001

3.2. FMP Y-maze test

TBI + vehicle treatment generally reduced % alternations and increased % repetitions in the Y-maze test ($p < 0.05$ vs control + vehicle group), whereas ISRIB treatment in the TBI + ISRIB fish group restored alternations to control + vehicle levels ($p < 0.05$ vs. TBI + vehicle group) and lowered repetitions ($p > 0.05$ vs. both TBI + vehicle and control + vehicle groups, Dunn's post-hoc test; Table 2). At the same time, ISRIB administered to the control + ISRIB fish did not affect these endpoints (Fig. 3). In general, higher percent of alternations (i.e., tetragrams RLRL + LRLR) and lower percent of repetitions (tetragrams RRRR + LLLL) reflect good working memory in this test (Cleal et al., 2021a,b).

3.3. Differential gene expression analysis

The effects of TBI and ISRIB on zebrafish brain transcriptomic responses (Fig. 4) were analyzed using RNA-sequencing with gene DE analyses and GSEA. We chose factorial (as opposed to group) analysis to ensure proper identification of interactions between the treatments. Preliminary PCA of DE genes supported moderate clusterization of control + vehicle, but not TBI + vehicle, control + ISRIB and TBI + ISRIB samples (Supplementary Fig. S1). Similarly, the heatmap diagram for all DE genes assayed supports weak separation of TBI + vehicle, control + ISRIB and TBI + ISRIB groups (Supplementary Fig. S2).

For DE analysis using DESeq2, three predictors were built in the negative binomial generalized linear model corresponding to factors TBI (yes/no), ISRIB (yes/no) and TBI x ISRIB interaction. Overall, we found 2432 DE genes (2217 up- and 215 downregulated; Supplementary Table S1) for TBI factor, 602 genes (540 up- and 62 downregulated; Supplementary Table S2) for ISRIB factor and 442 genes (30 up- and 412 downregulated; Supplementary Table S3) for interaction effect (Fig. 5). Genes were considered to be differentially expressed if their p-adjusted was < 0.05 and the $|\log2FoldChange| > 1$.

3.4. Gene set enrichment analysis (GSEA)

We further explored specific signaling biological pathways involved in neurotranscriptomic responses to TBI and/or ISRIB exposure using Proteins with Values/Ranks – Functional Enrichment Analysis available in the STRING database. Overall, we identified 446 enriched pathways (227 up-, 214 down- and 4 bidirectionally regulated. Supplementary Table S4) for ISRIB, 545 pathways (372 up-, 161 down-regulated, 12 bidirectional, Supplementary Table S5) for TBI and 324 pathways (108 up-, 212 down-, 4 bidirectional, Supplementary Table S6) for the interaction. All Gene Ontology (GO) pathways were further grouped into the parent categories for data representation and interpretation (Supplementary Tables S7-S9).

Fig. 7 and Supplementary Fig. S8 show the results of the customized GSEA performed on the 'ATF4 target genes' set. TBI factor notably upregulated this gene set ($p < 0.001$ GSEA), with multiple genes there

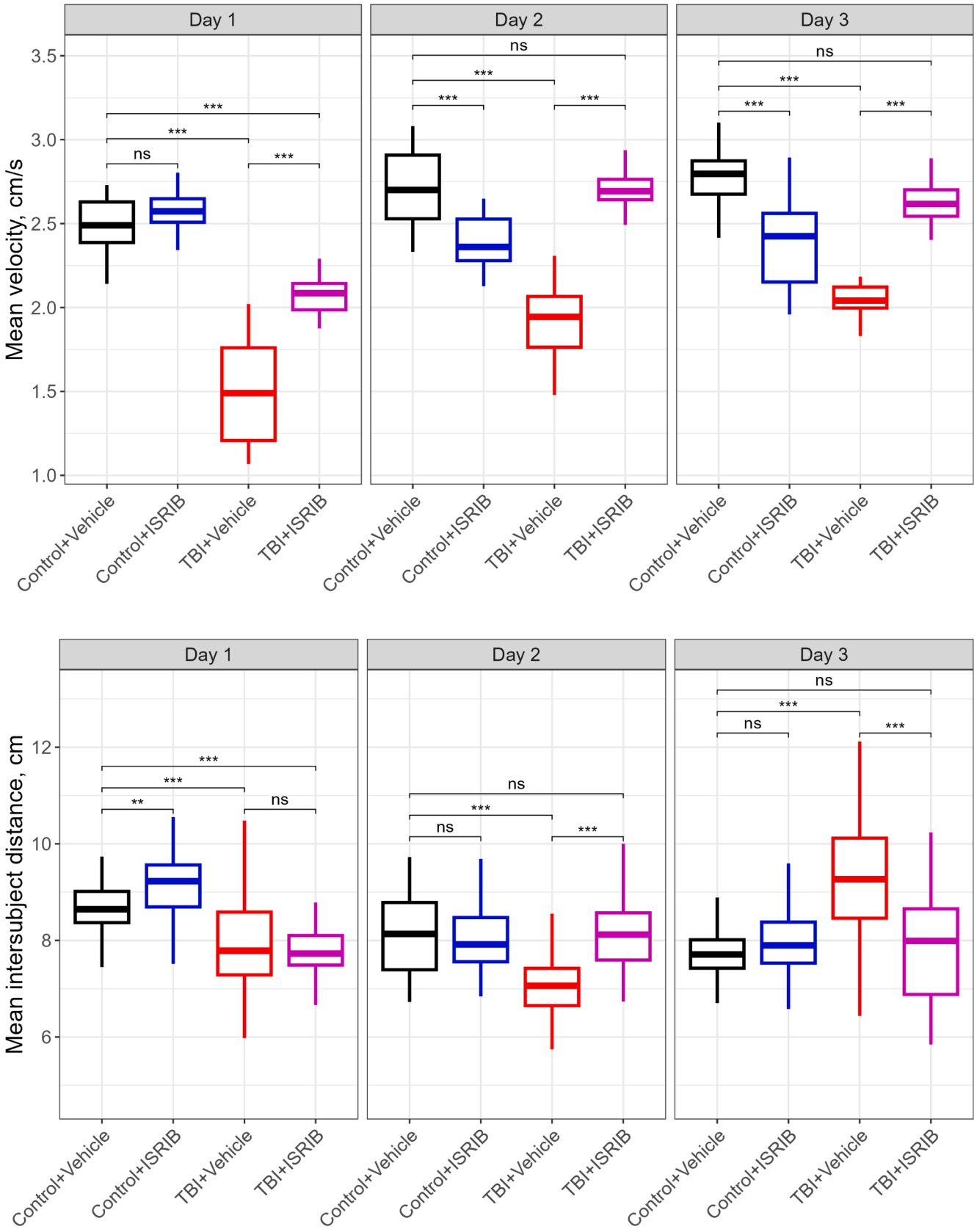

Fig. 2. Average velocity and average inter-fish distance in the zebrafish shoaling test on Days 1–3 post-injury (traumatic brain injury, TBI). ISRIB was injected i.p. on Days 0–2 post-injury, following behavioral testing. Each data point represents average distance between two animals during the test (fish were tested in groups of 10, with a total of 20 fish per group). Boxplots display the median, 25th and 75th percentiles, outliers are not shown. ***$p < 0.001$ (emmeans contrasts, with Sidak adjustment for multiple comparisons, n = 20 fish per group for velocity; total 90 distances for average inter-fish distance; see Table 1 for summary of statistical data).

Table 2
Summary of significant effects on zebrafish behavior in the Y-maze test determined by the Kruskal-Wallis test followed by post-hoc Dunn's test for pairwise comparisons.

Relative alternations, %			
Kruskal-Wallis chi-squared = 26.612, df = 3, p-value = 7.099e-06			
Comparison	Z	p	p. adj
Control + vehicle − Control + ISRIB	−0.57155	0.56763	1.00000
Control + vehicle − TBI + vehicle	4.01787	0.00006	0.00029
Control + ISRIB − TBI + vehicle	4.58942	0.00000	0.00003
Control + vehicle − TBI + ISRIB	0.11907	0.90522	0.90522
Control + ISRIB − TBI + ISRIB	0.69062	0.48980	1.00000
TBI + vehicle − TBI + ISRIB	−3.89879	0.00010	0.00039

Relative repetitions, %			
Kruskal-Wallis chi-squared = 16.88, df = 3, p-value = 0.0007479			
Comparison	Z	p	p. adj
Control + vehicle − Control + ISRIB	0.65320	0.51363	0.51363
Control + vehicle − TBI + vehicle	−3.18436	0.00145	0.00725
Control + ISRIB − TBI + vehicle	−3.83756	0.00012	0.00075
Control + vehicle − TBI + ISRIB	−0.73485	0.46243	0.92486
Control + ISRIB − TBI + ISRIB	−1.38805	0.16512	0.49536
TBI + vehicle − TBI + ISRIB	2.44950	0.01431	0.05722

also showing significant changes in expression based on differential gene expression analyses ($q < 0.001$, Fig. 7). In contrast, the set was significantly downregulated by the Interaction factor ($p < 0.001$), whereas no significant enrichment, either positive or negative, was observed under the ISRIB factor ($p > 0.05$, Fig. 7).

3.5. WGCNA co-expression network

We next applied WGCNA to identify small sets of genes with similar co-expression patterns for TBI and ISRIB without interaction. From 23 identified co-expression modules, 9 were deemed significant between TBI and ISRIB factors (Fig. 5). To evaluate the nature of the identified networks, we applied the clusterProfiler GSEA for GO and KEGG on genes from the submitted modules. The GO results confirmed that modular genes positively loading on TBI represent pathways associated with immune response, inflammation, cellular division, and DNA repair, whereas modular genes positively loading on ISRIB are associated with neuroplasticity, morphogenesis, synapse and vesicles organization pathways (Supplementary Fig. S4-S7). Finally, our KEGG analyses linked TBI to apoptosis, cell cycle, DNA repair and replication, necroptosis and cytokine pathways (Supplementary Fig. S4-S7).

Additionally, we also assessed module-module relationships using the Spearman correlation (Supplementary Fig. S3). Expectedly, multiple modules with similar functional characteristics positively correlated in the present study, supporting the validity of WGCNA applied here. As shown in this figure, gene clusters with highest correlations (red and blue) are all associated with the TBI effect, whereas other clusters (brown and turquoise) both correlated and related to ISRIB effect.

4. Discussion

As already mentioned, ISRIB is a small-molecule inhibitor of the ISR signaling pathway that mitigates negative effects of eIF2α phosphorylation on protein translation (Sidrauski et al., 2013). The drug has shown promising results in various rodent models of neurotrauma, suggesting that ISR hyperactivation may indeed play a role in TBI pathogenesis. Furthermore, ISRIB reverses cognitive deficits induced by focal and diffuse TBI in mice (Chou et al., 2017), improves structural integrity of white matter in a controlled cortical impact rat TBI model (Zhou et al., 2023), reverses aberrant dendritic spine dynamics following concussive injury in mice (Frias et al., 2022), and lowers neuroinflammation induced in rats by surgical brain injury (Huang et al., 2021).

Expanding this field of research across taxa, our study is the first report evaluating therapeutic potential of ISRIB in a non-mammalian TBI model and focusing on its effects in both injured and normal controls. Compared to mammals, zebrafish possess higher potential to regenerate neural tissue, hence enabling complete recovery following TBI in a relatively short period of time (März et al., 2011, Schmidt et al., 2014). Overall, telencephalic injury in our TBI model resulted in hypolocomotor profile on all 3 days. In contrast, these motor deficits were effectively rescued by ISRIB in the TBI + ISRIB group. Unexpectedly, control + ISRIB treatment in normal fish also induced hypolocomotion on Days 2 and 3, suggesting its time-dependent and potentially 'calming' effects on zebrafish locomotor behavior.

Increased shoaling behavior following telencephalic TBI + vehicle on Days 1 and 2 post-injury may be attributed to a higher anxiety level in zebrafish in this test (see (Maximino et al., 2010) for details), whereas opposite behavior on Day 3 may reflect a recovery phase or adaptation.

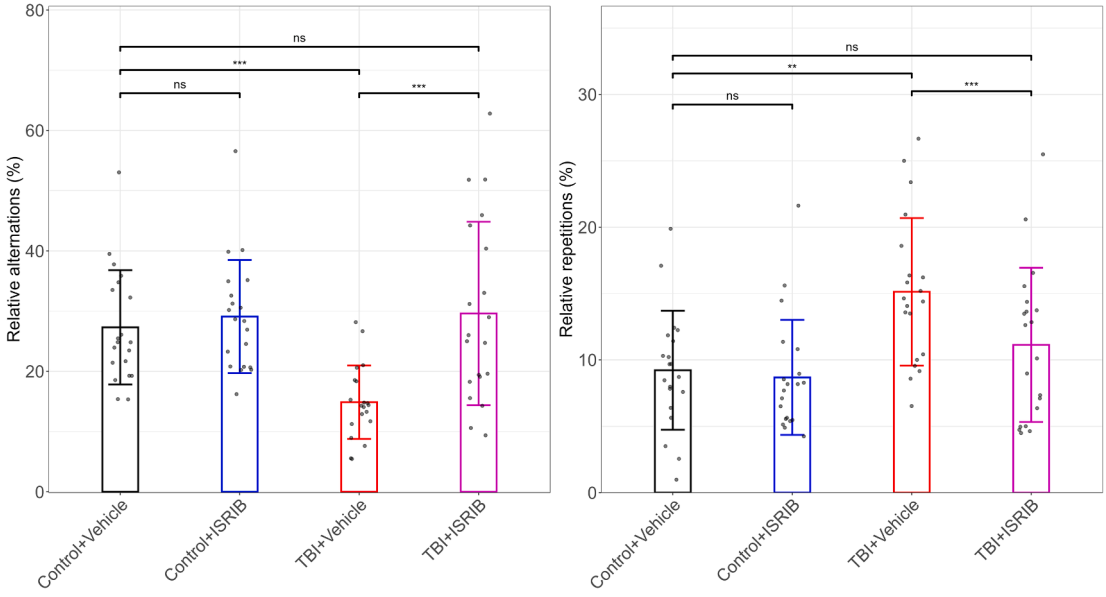

Fig. 3. Effects of traumatic brain injury (TBI) and ISRIB i.p. injections on zebrafish behavior in the Y-maze test on Day 3 post-injury (traumatic brain injury, TBI). Data are presented as mean ± SD (standard deviation of mean). **p < 0.01, ***p < 0.001, Dunn's post-hoc pairwise comparisons for significant Kruskal-Wallis data (n = 20 per group; see Tables 3 and 4 for details, and Table 2 for summary of statistical data).

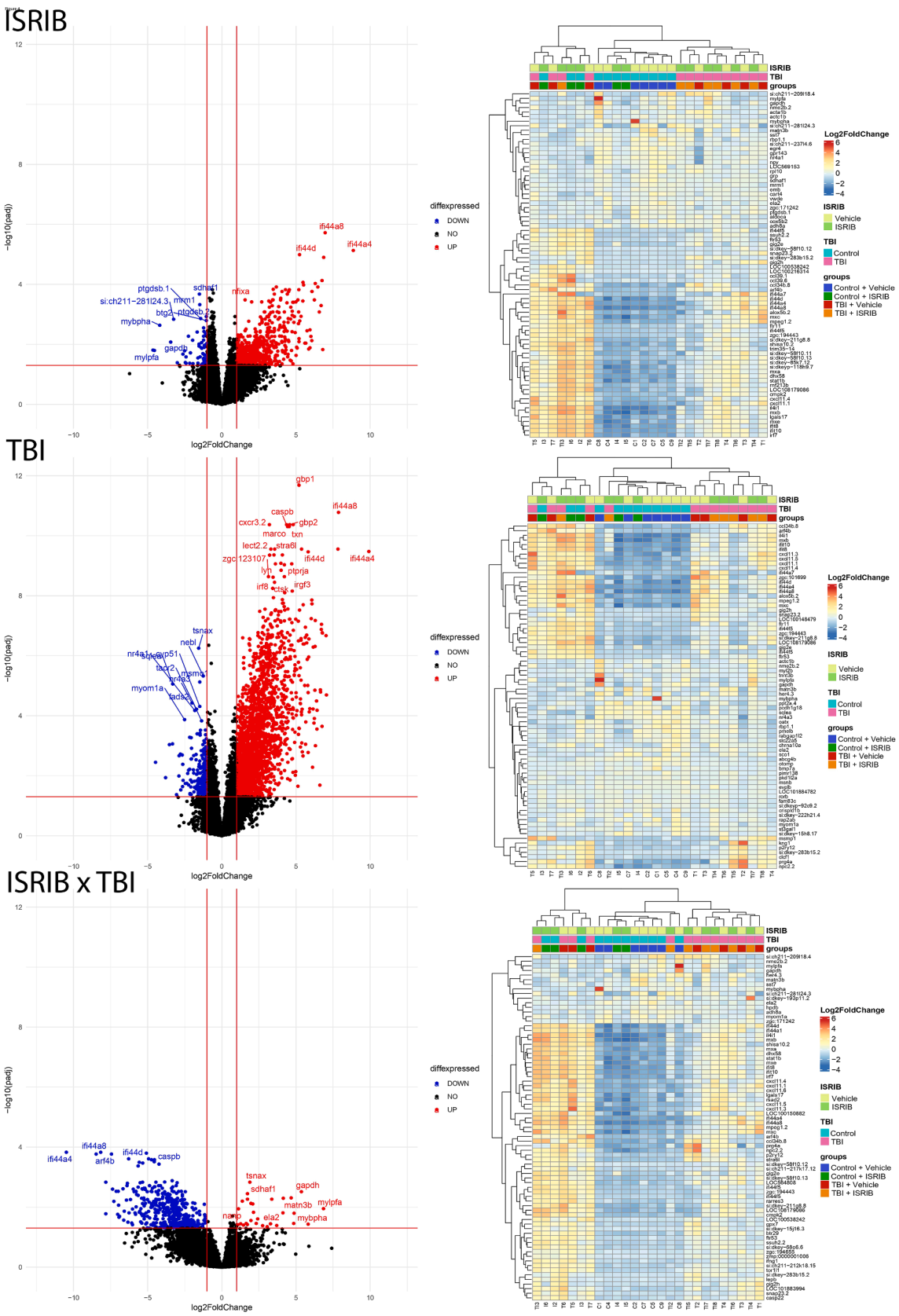

Fig. 4. Volcano plots for differentially expressed genes in zebrafish brain samples (left) and top 80 differentially expressed genes for each factor (right). ISRIB x TBI corresponds to the interaction of ISRIB treatment and traumatic brain injury (TBI).

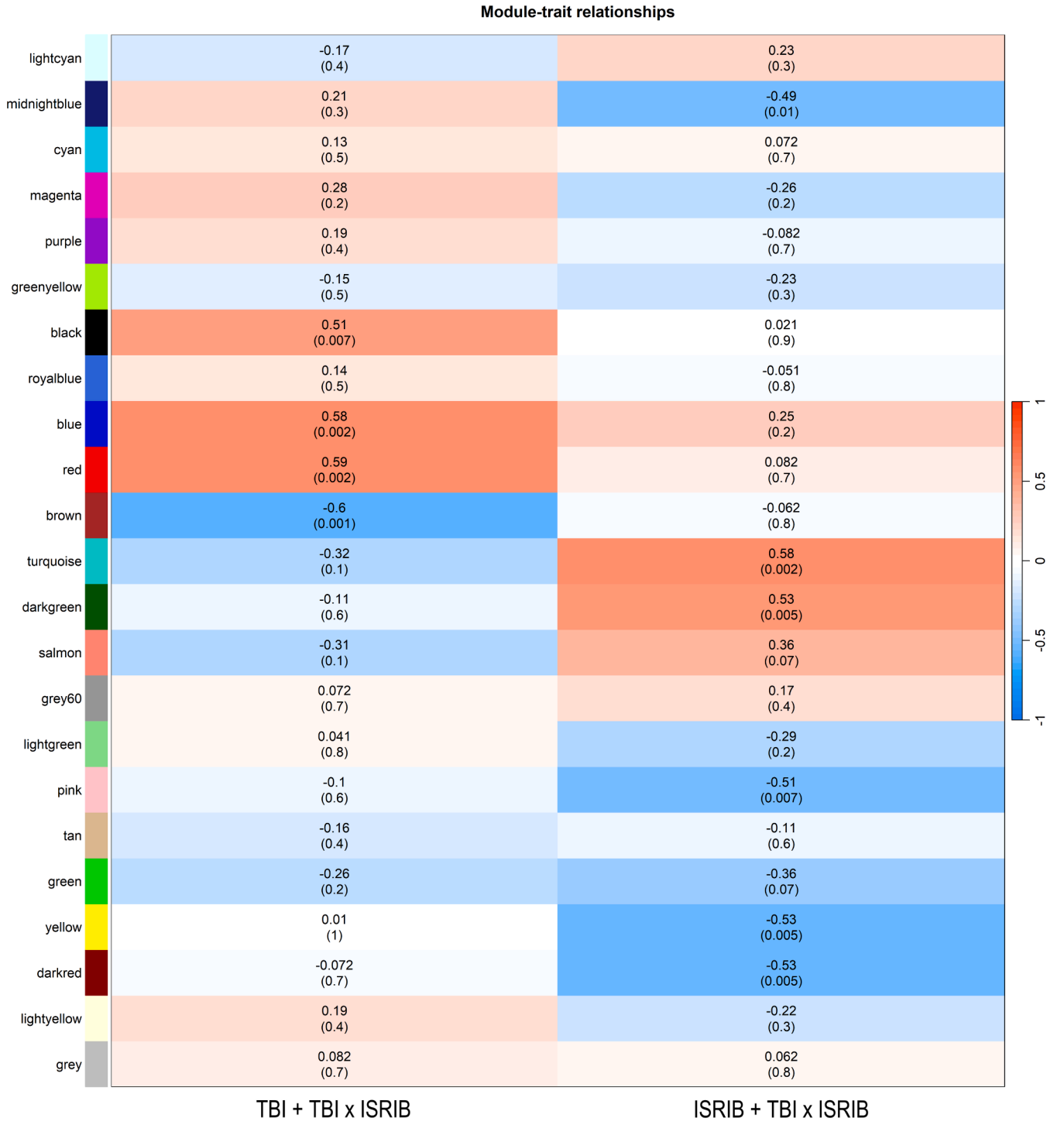

Fig. 5. Correlation plot of gene co-expression network. The x-axis represents the condition of samples (for interpretation of color in this figure, the reader is referred to the web version of this article).

Interestingly, the TBI + ISRIB treatment effectively normalized these parameters on both Days 2 (reducing higher shoaling) and 3 (recovering looser shoaling), indicating its potential therapeutic role in mitigating social behavioral deficits induced by TBI + vehicle at various time points. ISRIB injections to control + ISRIB fish induced distinct effects on shoaling behavior, increasing it on Day 1, but not on Days 2–3, further supporting its time-dependent CNS action, potentially reflecting behavioral adaptations following a chronic exposure.

The Y-maze testing on Day 3 post-TBI revealed significant effects of TBI + vehicle on zebrafish cognitive functions, since fewer alternations and more repetitions (Fig. 2) in this test indicate poorer spatial working memory (Cleal et al., 2021a,b, Cleal et al., 2022). Cognitive functions in general, and working memory in particular, are commonly disrupted in various TBI studies (Mcallister et al., 2004, Hoskison et al., 2009, Kobori et al., 2015), including both zebrafish (Hentig et al., 2021, Chaoul et al., 2022) and humans (Dunning et al., 2016, Phillips et al., 2017). ISRIB treatment in TBI + ISRIB fish effectively restored the percentage of spontaneous alternations to control + vehicle levels and partially

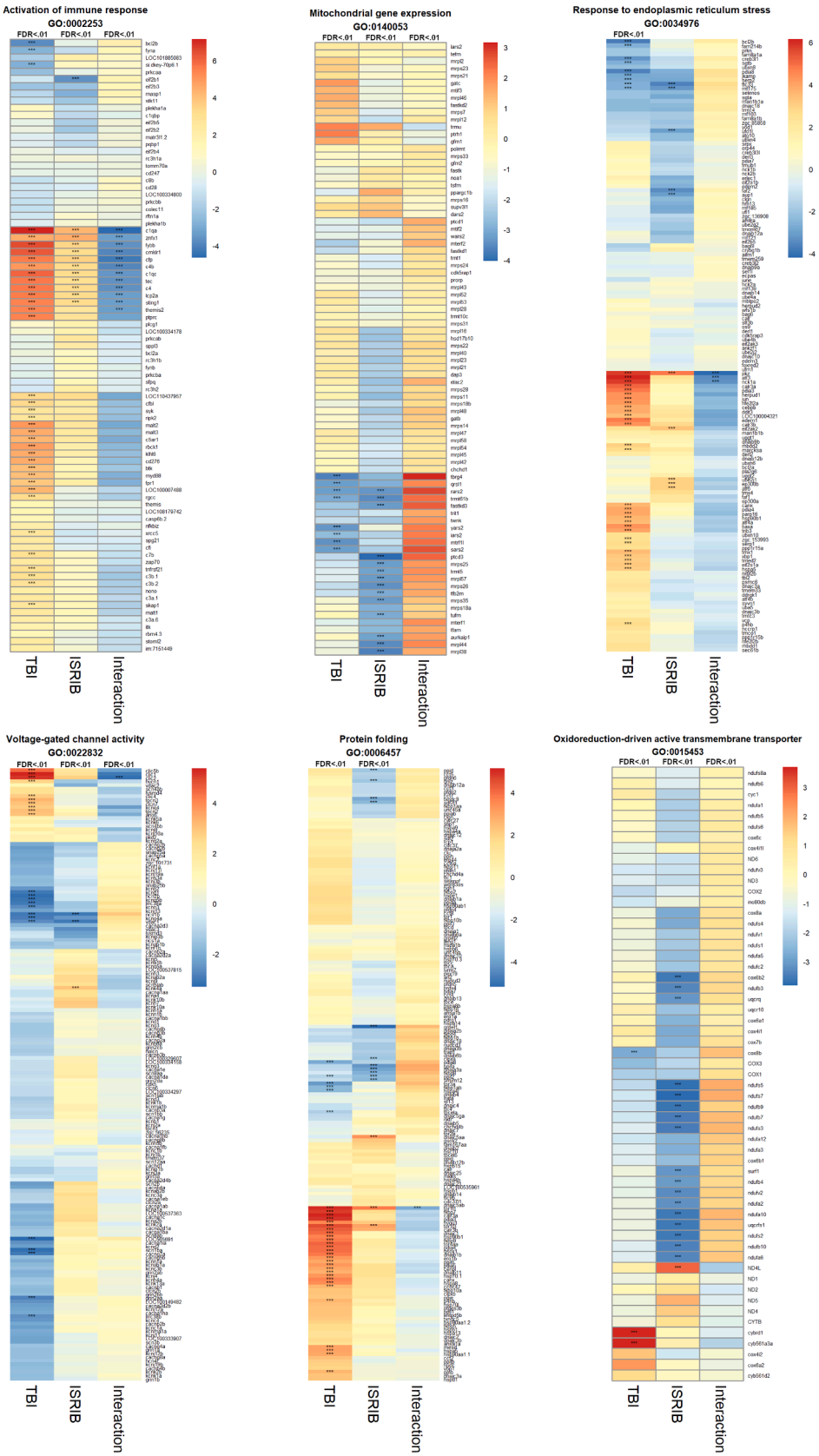

Fig. 6. Heatmaps representing l2fc for genes (based on DESeq2 data) constituting the Genetic Ontology (GO) pathways found to be enriched in the present study using the Gene Set Enrichment Analysis (GSEA). L2fc is presented relative to control + vehicle factor. Note high heterogeneity of expression profiles between the factors. ***p.adj < 0.001 is for DESeq2 comparison of a gene of corresponding factor to control + vehicle factor (for interpretation of color in this figure, the reader is referred to the web version of this article). The false discovery rate (FDR) < 0.01 for statistically significant set enrichment based on GSEA analysis relative to null distribution (see the Methods sections for details).

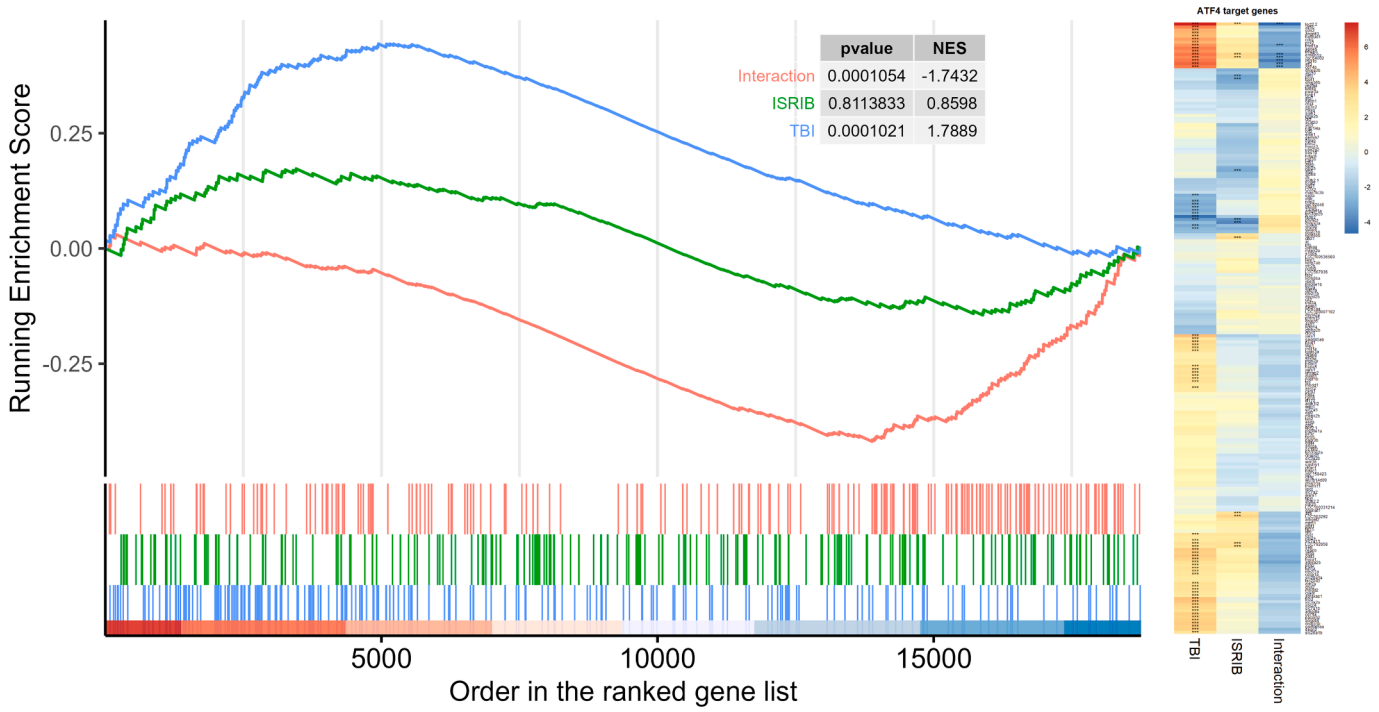

Fig. 7. Results of a custom Gene Set Enrichment Analysis (GSEA) of a set of putative ATF4 target genes across three ranked gene lists for TBI, ISRIB, and their interaction. The list of putative ATF4 target genes was obtained from a recent study that compiled the existent ChiP and chromatin immunoprecipitation data in mammalian species (Neill and Masson 2023). Zebrafish orthologues of those genes were next acquired using the g:Profiler web-resource (https://biit.cs.ut.ee/gprofiler/orth). Left panel displays the distribution of putative ATF4-target genes across the ranked gene lists (bottom) and the running enrichment score for each GSEA analysis (top). The accompanying table on the left plot shows p-values (<0.001 considered significant) and normalized enrichment scores (NES, enrichment score adjusted for gene set size). A positive NES suggests that genes in the list tend to cluster towards the top, while a negative NES indicates a tendency to cluster towards the bottom, of the list. Right plot is heatmap representing l2fc for genes constituting custom ATF4-downstream pathway. ***p.adj < 0.001 is for DESeq2 comparison of a gene of corresponding factor to control + vehicle factor (see the Methods section for details; for interpretation of color in this figure, the reader is referred to the web version of this article).

normalized repetitions, hence demonstrating potential procognitive effects of this drug. Notably, these results are also in line with rodent data, where ISRIB similarly improves cognitive performance impaired by TBI (Frias et al., 2022). In contrast, administered to healthy fish, control + ISRIB did not affect any working memory parameters assessed here (Fig. 2). Interestingly, as ISRIB improves spatial and fear-associated learning in healthy mice, it was speculated that some cognitive functions may be inherently limited by ISR (Sidrauski et al., 2013). However, while based on different testing paradigms applied here, our findings do not afford direct comparisons of ISRIB effects on memory in mice vs. zebrafish, these findings are interesting, and corroborate current trend in humans to use ISRIB as a cognitive enhancer, marketed online in various countries as a nootropic agent (e.g., https://www.simplynootropics.com.au, https://www.redpillnootrop.ru/isrib/).

Functional enrichment analysis of RNA sequencing data revealed multiple GO pathways bidirectionally modulated by TBI in zebrafish, which can be further categorized into several clusters. Specifically, TBI induced significant upregulation of inflammation-related pathways, encompassing various aspects of immune system processes, such as immune cell activation and differentiation, toll-like receptor signaling, complement activation, as well as cytokine- and chemokine-mediated signaling. TBI also upregulated pathways related to programmed cell death/apoptosis, and cysteine-type endopeptidases involved in the latter, suggesting apoptosis as a key early-stage response to brain injury in zebrafish. In line with this, the zebrafish orthologue of pro-survival gene *BCL2* in the apoptotic pathway was also downregulated in the present study. Other pathways upregulated by TBI include DNA replication, chromosome segregation, and cell division, suggesting extensive cell proliferation following neurotrauma. Although it is unclear which cells undergo division, the early post-injury state and the lack of enriched neurogenesis-related pathways implicate proliferation of immune cells (rather than neuronal precursors).

At the same time, TBI downregulated pathways involved in nerve impulse conduction, such as synapse organization, voltage-gated cation channel activity, and neurotransmitter receptor activity. TBI also suppressed the expression of genes encoding subunits of ionotropic glutamate and gamma-aminobutyric acid (GABA)-A receptors, as well as some serotonin, dopamine and histamine receptors, suggesting disrupted neuronal functioning potentially contributing to the observed behavioral defects here. Reduced expression of ionotropic glutamate receptors and voltage-gated calcium channels may also be associated with a cellular 'defense' response to excitotoxicity, whereas the suppression of mitochondrial genes, particularly those encoding components of the respiratory chain, underscores the likely impact of TBI on cellular energy metabolism in the brain.

Interestingly, ISRIB treatment positively affected the expression of multiple 'immune' genes, leading to the enrichment of pathways related to inflammatory response, cytokine-mediated signaling and activation of immune cells. Moreover, ISRIB upregulated cysteine-type endopeptidase pathway, including apoptosis-related caspase genes *casp22* and *caspb*. To the best of our knowledge, these effects of ISRIB have not been reported previously, and their underlying mechanisms may involve either unknown off-target effects or a direct action of ISR inhibition on the immune system. Since most studies on ISRIB assess its effects in pathological conditions, our findings highlight its alternative (and potentially detrimental) effects on healthy organisms.

Likewise, ISRIB upregulated several pathways involved in neurogenesis and neuronal system development, including axonogenesis and neural crest cell development. The enrichment of these pathways was mainly due to the upregulation of genes encoding semaphorin and

plexin protein families, such as *sema4ba, plxnb2b, sema6e and plxna3*. In line with this, GO terms like semaphorin-plexin signaling pathway, semaphorin receptor binding, and semaphorin receptor activity show marked upregulation in the ISRIB fish brain. Semaphorins are secreted and membrane-bound proteins, whereas plexins are their receptors (Nogi et al., 2010), both essential for neurogenesis, including axonal guidance, neuronal migration, and synapse formation (Carulli et al., 2021, Limoni and Niquille 2021).

Another interesting finding is the upregulation of the Notch signaling pathway, with the zebrafish orthologs of the human Notch 1 receptor (*notch1b*) and DTX3L protein (*si:dkey-40c23.2.*) showing the highest change in gene expression levels, paralleling previous studies in the retinal toxicity model utilizing human retinal organoids (Rosarda et al., 2023). Importantly, Notch signaling plays a key role in injury-induced neurogenesis in both mammals and zebrafish, guiding the cell fate determination of neuronal stem cells (Kishimoto et al., 2012, Zhang et al., 2014, Ran et al., 2015). In zebrafish, *notch1b* is expressed specifically in activated neuronal progenitor cells (Alunni et al., 2013, Than-Trong et al., 2018). Furthermore, ISRIB treatment produced upregulation of pathways associated with normal neural functioning, such as synapse organization, voltage-gated channel activity, and vesicle-mediated transport in synapse, which were downregulated under TBI. Taken together, these findings may explain the observed positive behavioral effects of ISRIB in our TBI model and clarify some molecular mechanisms of ISRIB-induced neuroprotection.

We also expected that the activation of Notch pathway in control + ISRIB group can likely facilitate neuronal functioning (including motor neuron function), hence enhancing fish locomotor ability. Studies in other vertebrate models link the activation of Notch pathway to improved regeneration of motor neurons after injury (Dias et al., 2012, Kong et al., 2018). ISRIB injection in the present study also upregulated the expression of ionotropic glutamate receptors and voltage-gated calcium channels, which too may impact locomotor behavior. Contrary to our expectations, ISRIB lowered motor activity in the control + ISRIB group – the effect that can be related to downregulated mitochondrial genes, hence reducing neuronal bioenergetics, especially since mutations in some mitochondrial genes (e.g., SOD1) can lead to impaired motor activity and axonal transport, and degeneration of motor neurons (Song et al., 2013).

Among the pathways negatively regulated by ISRIB here, the largest group related to mitochondrial function, such as mitochondrial gene expression, mitochondrial respiratory chain complex assembly, and cellular respiration. This downregulation appears to be nonspecific, affecting multiple genes encoding mitochondrial ribosomal proteins, components of the electron transport chain, subunits of ATP synthase, mitochondrial inner and outer membrane translocases. Moreover, functional enrichment analysis using the KEGG database revealed downregulation of pathways involved in the metabolism of carbohydrates, amino acids, and fatty acids. While the exact mechanisms of this phenomenon are poorly understood, a remarkably similar effect of ISRIB on mitochondrial gene expression has been observed in human retinal cells (Rosarda et al., 2023), implying the existence of an evolutionarily conserved link between ISR inhibition and mitochondrial function.

Other pathways suppressed by ISRIB treatment are associated with protein synthesis, including transcription by RNA polymerase II, RNA processing, synthesis of tRNA, biogenesis of ribosomes, and translation initiation. Notably, ISRIB suppressed the gene expression of several subunits of the eukaryotic translation initiation complex, including its molecular target eIF2B (*eif2b1*). Taken together, these findings imply a negative effect of ISRIB on cellular metabolism. While ISRIB is known to activate ISR-suppressed protein translation and facilitate metabolic processes, its downstream effects on gene expression, particularly in healthy organisms, remain unclear. Our findings suggest that ISRIB-induced activation of translation may downregulate genes involved in cellular metabolism.

Interestingly, these findings suggest that TBI and ISRIB also exhibit complex interactions, with nonlinear relationship that can only be assessed when both factors are assessed. One possibility is that ISRIB has a differential effect in TBI vs. healthy fish, supporting the importance of two-factorial analyses of its effects in vivo. Such interactions involve multiple pathways that were unidirectionally altered by TBI and ISRIB, but in opposite directions by their interaction, suggesting that ISRIB beneficial effects may not be fully observed without neurotrauma. On the one hand, and rather expectedly, TBI x ISRIB interaction reduced enrichment in gene pathways involved in inflammatory responses, cytokine signaling, macrophage and T-cell activation, apoptosis and other related pathways, suggesting a potential anti-inflammatory ISRIB effect in TBI. Other pathways with reduced enrichment involved NF-kB and ERK activity, suggesting that these anti-inflammatory effects may be mediated via eIF2α dephosphorylation by ISRIB.

On the other hand, the interaction seems to positively affect cell respiratory and metabolic functions, increasing enrichment in mitochondrial respiratory chain complex assembly, aerobic respiration, amino acid catabolism, ubiquinone biosynthesis, amino acid degradation and other related pathways. Interaction also increased enrichment in pathways related to neuronal synaptic and membrane activity, including glutamatergic signaling, suggesting remodeling of glutamatergic pathways that can potentially protect from glutamatergic excitotoxicity. Finally, several enriched pathways implicate hormonal signaling in TBI x ISRIB interaction, including cellular response to corticotropin-releasing hormone, and estrogen biosynthesis. Thus, the TBI x ISRIB interaction effect primarily downregulated genes involved in inflammation and cell replication, and upregulated genes involved in neuronal signaling and cell respiration, further supporting ISRIB beneficial effects in neurotrauma, but also pointing to its less prominent effects on these genes without TBI.

We also observed a marked upregulation of the putative ATF4 target genes by TBI in zebrafish – the effect that was reversed by TBI x ISRIB interaction, but not ISRIB alone (Fig. 7; Supplementary Fig. S8). This finding suggests that ISRIB exerted a negative effect on the ATF4-mediated gene expression in TBI-exposed zebrafish, but not in healthy fish. At the same time, the upregulation of these genes by TBI links the observed TBI-induced changes in gene expression to the activation of ISR. These data further support the notion that TBI and ISRIB effects are at least partially mediated through *atf4* activity in zebrafish brain. Specific ATF4 target genes that increased their expression for TBI factor, but decreased their activity for the interaction, include *leukocyte cell derived chemotaxin 2.2* (*lect2.2*), *formin-like 1a* (*fmnl1a*), *TNF-alpha induced protein 6* (*tnfaip6*), *elastin microfibril interfacer 1a* (*emilin1a*), *activating transcription factor 3* (*atf3*) and *CD74 molecule, major histocompatibility complex,* and *class II invariant chain b* (*cd74b*) genes, all strongly implicated in inflammatory response and cell migration. Furthermore, we also constructed a protein–protein interaction (PPI) network consisting of key proteins involved in ISR signaling, based on (Pakos-Zebrucka et al., 2016), as shown in Supplementary Fig. S9. Overall, only *atf4a* altered brain expression following TBI in this PPI network. The expression of *atf4a* is typically controlled by the activation of ISR, elevating phosphorylated eIF2α, thus likely representing a potentially useful 'proxy' biomarker of ISR activity in our study. Notably, both ISRIB and TBI + ISRIB downregulated most of the ISR-related genes in the pathway vs. TBI, and recovered *atf4a* expression to control levels, suggesting normalized ISR activity following ISRIB treatment.

Notably, zebrafish also exhibit sex-specific DE brain genes, especially steroidogenic genes (Zhai et al., 2022). Although the present study did not address sex-specific effects of ISRIB activity, endocrine signaling may potentially differentially affect the TBI-ISRIB interaction in male vs. female fish. As not examining sex as a separate biological variable here represents a limitation of our study, future studies may assess potential sex-specific effects of ISRIB in zebrafish TBI models in detail, aiming to better understand how hormonal signaling may distinctly impact CNS ISR-related processes across sexes. Another study limitation is that we

did not monitor individual recovery trajectories in zebrafish following TBI and did not correlate RNA-seq results to behavioral data. As such, follow-up studies may assess individual variance in both TBI- and ISRIB-evoked zebrafish CNS responses. Likewise, we only examined one age (adult zebrafish) and one strain in the present study, warranting further studies into TBI and ISRIB effects across the lifespan, and in a wider range of zebrafish strains, in order to extend the overall generality of the present findings.

As adult zebrafish have great capacity for neural restoration following TBI, this also raises the question of whether the addition of ISRIB would influence the ultimate recovery of zebrafish here. Because brain structure and function are completely restored in zebrafish following a 1-month recovery in the telencephalic TBI model (Kishimoto et al., 2012), ISRIB would probably not affect final phenotype per se, but may clearly facilitate the recovery by reducing the initial neuroinflammation, warranting further studies. Finally, while there was a substantial overlap in functional pathways enriched between all three factors (ISRIB, TBI and interaction), the specific DE genes involved in these pathways differed for each factor (Fig. 6). For example, for activation of the immune response, 11 DE genes were shared by all three factors (upregulated in ISRIB and TBI, but downregulated in interaction), whereas TBI had 23 additional up- and 3 down-regulated genes from this pathway. Similarly, both ISRIB and TBI downregulated mitochondrial gene expression, yet only 2 genes were jointly downregulated in this pathway. Overall, this suggests that while TBI and ISRIB have overlapping neurotranscriptomic profiles, they likely involve distinct molecular and cellular mechanisms.

In conclusion, our study reports overt neurogenomic and behavioral changes induced by telencephalic TBI in adult zebrafish, including locomotor, social behavior and working memory deficits. We demonstrated, for the first time, that ISRIB can normalize TBI-induced changes in a non-mammalian model (zebrafish), suggesting that the ISR hyperactivation via eIF2α phosphorylation may indeed represent a common, evolutionarily conserved mechanism that hinders brain recovery after injury. We also noted some effects of ISRIB on CNS gene expression in healthy zebrafish, showing its rather limited beneficial activity alone, without TBI. Finally, our findings suggest zebrafish as a valuable and sensitive model for studying mechanisms of ISR-related neuropathologies in general, and for developing therapeutic interventions based on targeting the ISR signaling pathway.

CRediT authorship contribution statement

Nikita P. Ilyin: Writing – review & editing, Writing – original draft, Visualization, Methodology, Investigation, Formal analysis. **Anton D. Shevlyakov:** Writing – original draft, Formal analysis. **Galina A. Boyko:** Writing – original draft, Investigation. **Anastasia M. Moskalenko:** Writing – original draft, Investigation. **Aleksey N. Ikrin:** Writing – original draft, Investigation. **David S. Galstyan:** Writing – original draft, Investigation, Conceptualization. **Tatiana O. Kolesnikova:** Writing – original draft, Investigation. **Nataliia V. Katolikova:** Writing – original draft, Investigation. **Sergei A. Chekrygin:** Writing – original draft, Investigation. **Lee Wei Lim:** Writing – original draft, Investigation. **LongEn Yang:** Writing – original draft, Investigation. **Murilo S. De Abreu:** Writing – original draft, Investigation. **Konstantin B. Yenkoyan:** Writing – review & editing, Investigation. **Allan V. Kalueff:** Writing – review & editing, Validation, Supervision, Resources, Project administration, Funding acquisition. **Konstantin A. Demin:** Writing – review & editing, Writing – original draft, Validation, Supervision, Resources, Project administration, Methodology, Funding acquisition, Data curation, Conceptualization.

Declaration of competing interest

The authors declare that they have no known competing financial interests or personal relationships that could have appeared to influence the work reported in this paper. N.P.I. and D.S.G. received support by St. Petersburg State University.

Acknowledgements

The project was supported by the Ministry of Science and Higher Education of Russian Federation (Agreement No. 075-15-2022-301).

Appendix A. Supplementary data

Supplementary data to this article can be found online at https://doi.org/10.1016/j.brainres.2024.149329.

Data availability

All transcriptomic data, including the script used for it analysis is available from the repositories links mentioned in the manuscript.

References

Aldag, M., Armstrong, R.C., Bandak, F., Bellgowan, P.S.F., Bentley, T., Biggerstaff, S., Caravelli, K., Cmarik, J., Crowder, A., DeGraba, T.J., Dittmer, T.A., Ellenbogen, R.G., Greene, C., Gupta, R.K., Hicks, R., Hoffman, S., Latta, R.C., Leggieri, M.J., Marion, D., Mazzoli, R., McCrea, M., O'Donnell, J., Packer, M., Petro, J.B., Rasmussen, T.E., Sammons-Jackson, W., Shoge, R., Tepe, V., Tremaine, L.A., Zheng, J., 2017. The biological basis of chronic traumatic encephalopathy following blast injury: a literature review. J. Neurotrauma 34 (S1), S-26–S–43.

Alunni, A., Krecsmarik, M., Bosco, A., Galant, S., Pan, L., Moens, C.B., Bally-Cuif, L., 2013. Notch3 signaling gates cell cycle entry and limits neural stem cell amplification in the adult pallium. Development 140 (16), 3335–3347.

B'chir, W., Maurin, A.-C., Carraro, V., Averous, J., Jousse, C., Muranishi, Y., Parry, L., Stepien, G., Fafournoux, P., Bruhat, A., 2013. The eIF2α/ATF4 pathway is essential for stress-induced autophagy gene expression. Nucleic Acids Res. 41 (16), 7683–7699.

Bashirzade, A.A., Zabegalov, K.N., Volgin, A.D., Belova, A.S., Demin, K.A., de Abreu, M. S., Babchenko, V.Y., Bashirzade, K.A., Yenkoyan, K.B., Tikhonova, M.A., 2022. Modeling neurodegenerative disorders in zebrafish. Neurosci. Biobehav. Rev. 138, 104679.

Begum, G., Yan, H.Q., Li, L., Singh, A., Dixon, C.E., Sun, D., 2014. Docosahexaenoic acid reduces ER stress and abnormal protein accumulation and improves neuronal function following traumatic brain injury. J. Neurosci. 34 (10), 3743–3755.

Bolger, A.M., Lohse, M., Usadel, B., 2014. Trimmomatic: a flexible trimmer for Illumina sequence data. Bioinformatics 30 (15), 2114–2120.

Bond, S., Lopez-Lloreda, C., Gannon, P.J., Akay-Espinoza, C., Jordan-Sciutto, K.L., 2020. The integrated stress response and phosphorylated eukaryotic initiation factor 2α in neurodegeneration. J. Neuropathol. Exp. Neurol. 79 (2), 123–143.

Buffington, S.A., Huang, W., Costa-Mattioli, M., 2014. Translational Control in Synaptic Plasticity and Cognitive Dysfunction. Annu. Rev. Neurosci. 37 (1), 17–38.

Carulli, D., De Winter, F., Verhaagen, J., 2021. Semaphorins in adult nervous system plasticity and disease. Front. Synaptic Neurosci. 13, 672891.

Chaoul, V., Awad, M., Harb, F., Najjar, F., Hamade, A., Nabout, R., Soueid, J., 2022. Saffron Extract Attenuates Anxiogenic Effect and Improves Cognitive Behavior in an Adult Zebrafish Model of Traumatic Brain Injury. Int. J. Mol. Sci. 23 (19), 11600.

Chou, A., Krukowski, K., Jopson, T., Zhu, P.J., Costa-Mattioli, M., Walter, P., Rosi, S., 2017. Inhibition of the integrated stress response reverses cognitive deficits after traumatic brain injury. Proc. Natl. Acad. Sci. U.S.A. 114 (31).

Cleal, M., Fontana, B.D., Parker, M.O., 2021a. The cognitive and behavioral effects of D-amphetamine and nicotine sensitization in adult zebrafish. Psychopharmacology (Berl) 238 (8), 2191–2200.

Cleal, M., Fontana, B.D., Ranson, D.C., McBride, S.D., Swinny, J.D., Redhead, E.S., Parker, M.O., 2021b. The Free-movement pattern Y-maze: A cross-species measure of working memory and executive function. Behav. Res. Methods 53 (2), 536–557.

Cleal, M., Fontana, B.D., Hillman, C., Parker, M.O., 2022. Ontogeny of working memory and behavioural flexibility in the free movement pattern (FMP) Y-maze in zebrafish. Behav. Process. 212, 104943.

Coronado, V.G., McGuire, L.C., Faul, M., Sugerman, D.E., Pearson, W.S., 2012. Traumatic brain injury epidemiology and public health issues. Brain Injury Medicine: Principles and Practice 84, 84–100.

Costa-Mattioli, M., Walter, P., 2020. The integrated stress response: From mechanism to disease. Science 368 (6489), eaat5314.

Daneshvar, D.H., Riley, D.O., Nowinski, C.J., McKee, A.C., Stern, R.A., Cantu, R.C., 2011. Long-term consequences: effects on normal development profile after concussion. Phys. Med. Rehabil. Clin. 22 (4), 683–700.

Delic, V., Beck, K.D., Pang, K.C.H., Citron, B.A., 2020. Biological links between traumatic brain injury and Parkinson's disease. Acta Neuropathol. Commun. 8 (1), 45.

Demin, K.A., Lakstygal, A.M., Alekseeva, P.A., Sysoev, M., de Abreu, M.S., Alpyshov, E. T., Serikuly, N., Wang, D., Wang, M., Tang, Z., 2019. The role of intraspecies variation in fish neurobehavioral and neuropharmacological phenotypes in aquatic models. Aquat. Toxicol. 210, 44–55.

Demin, K.A., Lakstygal, A.M., Krotova, N.A., Masharsky, A., Tagawa, N., Chernysh, M.V., Ilyin, N.P., Taranov, A.S., Galstyan, D.S., Derzhavina, K.A., 2020. Understanding complex dynamics of behavioral, neurochemical and transcriptomic changes induced by prolonged chronic unpredictable stress in zebrafish. Sci. Rep. 10 (1), 19981.
Dewan, M.C., Rattani, A., Gupta, S., Baticulon, R.E., Hung, Y.-C., Punchak, M., Agrawal, A., Adeleye, A.O., Shrime, M.G., Rubiano, A.M., 2018. Estimating the global incidence of traumatic brain injury. J. Neurosurg. 130 (4), 1080–1097.
Di Domenico, F., Lanzillotta, C., 2022. The disturbance of protein synthesis/degradation homeostasis is a common trait of age-related neurodegenerative disorders. Adv. Protein Chem. Struct. Biol. 132, 49–87.
Dias, T.B., Yang, Y.-J., Ogai, K., Becker, T., Becker, C.G., 2012. Notch signaling controls generation of motor neurons in the lesioned spinal cord of adult zebrafish. J. Neurosci. 32 (9), 3245–3252.
Donnelly, N., Gorman, A.M., Gupta, S., Samali, A., 2013. The eIF2α kinases: their structures and functions. Cell. Mol. Life Sci. 70, 3493–3511.
Dunning, D.L., Westgate, B., Adlam, A.-L.-R., 2016. A meta-analysis of working memory impairments in survivors of moderate-to-severe traumatic brain injury. Neuropsychology 30 (7), 811.
Engeszer, R.E., Da Barbiano, L.A., Ryan, M.J., Parichy, D.M., 2007. Timing and plasticity of shoaling behaviour in the zebrafish, Danio rerio. Anim. Behav. 74 (5), 1269–1275.
Finkelstein, E., Corso, P.S., Miller, T.R., 2006. The incidence and economic burden of injuries in the United States. Oxford University Press.
Fontana, B.D., Cleal, M., Gibbon, A.J., McBride, S.D., Parker, M.O., 2021. The effects of two stressors on working memory and cognitive flexibility in zebrafish (Danio rerio): the protective role of D1/D5 agonist on stress responses. Neuropharmacology 196, 108681.
Frias, E.S., Hoseini, M.S., Krukowski, K., Paladini, M.S., Grue, K., Ureta, G., Rienecker, K. D.A., Walter, P., Stryker, M.P., Rosi, S., 2022. Aberrant cortical spine dynamics after concussive injury are reversed by integrated stress response inhibition. Proc. Natl. Acad. Sci. U.S.A. 119 (42), e2209427119.
Graves, A.B., White, E., Koepsell, T.D., Reifler, B.V., Van Belle, G., Larson, E.B., Raskind, M., 1990. The association between head trauma and Alzheimer's disease. Am. J. Epidemiol. 131 (3), 491–501.
Green, J., Collins, C., Kyzar, E.J., Pham, M., Roth, A., Gaikwad, S., Cachat, J., Stewart, A. M., Landsman, S., Grieco, F., 2012. Automated high-throughput neurophenotyping of zebrafish social behavior. J. Neurosci. Methods 210 (2), 266–271.
Guo, Z., Cupples, L.A., Kurz, A., Auerbach, S.H., Volicer, L., Chui, H., Green, R.C., Sadovnick, A.D., Duara, R., DeCarli, C., 2000. Head injury and the risk of AD in the MIRAGE study. Neurology 54 (6), 1316–1323.
Hentig, J., Cloghessy, K., Hyde, D.R., 2021. Shuttle box assay as an associative learning tool for cognitive assessment in learning and memory studies using adult zebrafish. J. Visual. Exper. 173, e62745.
Hinnebusch, A.G., 2005. Translational regulation of GCN4 and the general amino acid control of yeast. Annu. Rev. Microbiol. 59, 407–450.
Hoskison, M.M., Moore, A.N., Hu, B., Orsi, S., Kobori, N., Dash, P.K., 2009. Persistent working memory dysfunction following traumatic brain injury: evidence for a time-dependent mechanism. Neuroscience 159 (2), 483–491.
Huang, T.-C., Luo, L., Jiang, S.-H., Chen, C., He, H.-Y., Liang, C.-F., Li, W.-S., Wang, H., Zhu, L., Wang, K., et al., 2021. Targeting integrated stress response regulates microglial M1/M2 polarization and attenuates neuroinflammation following surgical brain injury in rat. Cell. Signal. 85, 110048.
Huber, W., Carey, V.J., Gentleman, R., Anders, S., Carlson, M., Carvalho, B.S., Bravo, H. C., Davis, S., Gatto, L., Girke, T., 2015. Orchestrating high-throughput genomic analysis with Bioconductor. Nat. Methods 12 (2), 115–121.
Jackson, R.J., Hellen, C.U.T., Pestova, T.V., 2010. The mechanism of eukaryotic translation initiation and principles of its regulation. Nat. Rev. Mol. Cell Biol. 11 (2), 113–127.
James, S.L., Theadom, A., Ellenbogen, R.G., Bannick, M.S., Montjoy-Venning, W., Lucchesi, L.R., Abbasi, N., Abdulkader, R., Abraha, H.N., Adsuar, J.C., 2019. Global, regional, and national burden of traumatic brain injury and spinal cord injury, 1990–2016: a systematic analysis for the Global Burden of Disease Study 2016. The Lancet Neurology 18 (1), 56–87.
Johnson, V.E., Stewart, W., Smith, D.H., 2010. Traumatic brain injury and amyloid-β pathology: a link to Alzheimer's disease? Nat. Rev. Neurosci. 11 (5), 361–370.
Kinkel, M.D., Eames, S.C., Philipson, L.H., Prince, V.E., 2010. Intraperitoneal injection into adult zebrafish. JoVE (Journal of Visualized Experiments) 42, e2126.
Kishimoto, N., Shimizu, K., Sawamoto, K., 2012. Neuronal regeneration in a zebrafish model of adult brain injury. Dis. Model. Mech. 5 (2), 200–209.
Kobori, N., Moore, A.N., Dash, P.K., 2015. Altered regulation of protein kinase a activity in the medial prefrontal cortex of normal and brain-injured animals actively engaged in a working memory task. J. Neurotrauma 32 (2), 139–148.
Kong, H.J., Ryu, J.-H., Kim, J., Kim, J.-W., Seong, B., Whang, I., Park, J.Y., Yeo, S.-Y., 2018. Generation of motor neurons requires spatiotemporal coordination between retinoic acid and Mib-mediated Notch signaling. Anim. Cells Syst 22 (2), 76–81.
Krukowski, K., Nolan, A., Frias, E.S., Grue, K., Becker, M., Ureta, G., Delgado, L., Bernales, S., Sohal, V.S., Walter, P., et al., 2020. Integrated stress response inhibitor reverses sex-dependent behavioral and cell-specific deficits after mild repetitive head trauma. J. Neurotrauma 37 (11), 1370–1380.
Langfelder, P., Horvath, S., 2008. WGCNA: an R package for weighted correlation network analysis. BMC Bioinf. 9, 1–13.
Limoni, G., Niquille, M., 2021. Semaphorins and Plexins in central nervous system patterning: the key to it all? Curr. Opin. Neurobiol. 66, 224–232.
Love, M.I., Huber, W., Anders, S., 2014. Moderated estimation of fold change and dispersion for RNA-seq data with DESeq2. Genome Biol. 15, 1–21.
März, M., Schmidt, R., Rastegar, S., Strähle, U., 2011. Regenerative response following stab injury in the adult zebrafish telencephalon. Dev. Dyn. 240 (9), 2221–2231.
Maximino, C., de Brito, T.M., da Silva Batista, A.W., Herculano, A.M., Morato, S., Gouveia Jr, A., 2010. Measuring anxiety in zebrafish: a critical review. Behav. Brain Res. 214 (2), 157–171.
Mcallister, T.W., Flashman, L.A., Sparling, M.B., Saykin, A.J., 2004. Working memory deficits after traumatic brain injury: catecholaminergic mechanisms and prospects for treatment—a review. Brain Inj. 18 (4), 331–350.
Menon, D.K., Schwab, K., Wright, D.W., Maas, A.I., 2010. Position statement: definition of traumatic brain injury. Arch. Phys. Med. Rehabil. 91 (11), 1637–1640.
Meshalkina, D.A., Kysil, E.V., Warnick, J.E., Demin, K.A., Kalueff, A.V., 2017. Adult zebrafish in CNS disease modeling: a tank that's half-full, not half-empty, and still filling. Lab Anim. 46 (10), 378–387.
Mortimer, J.A., French, L.R., Hutton, J.T., Schuman, L.M., 1985. Head injury as a risk factor for Alzheimer's disease. Neurology 35 (2), 264.
Neill, G., Masson, G.R., 2023. A stay of execution: ATF4 regulation and potential outcomes for the integrated stress response. Front. Mol. Neurosci. 16, 1112253.
Nogi, T., Yasui, N., Mihara, E., Matsunaga, Y., Noda, M., Yamashita, N., Toyofuku, T., Uchiyama, S., Goshima, Y., Kumanogoh, A., 2010. Structural basis for semaphorin signalling through the plexin receptor. Nature 467 (7319), 1123–1127.
Ohno, M., 2014. Roles of eIF2α kinases in the pathogenesis of Alzheimer's disease. Front. Mol. Neurosci. 7, 22.
Pakos-Zebrucka, K., Koryga, I., Mnich, K., Ljujic, M., Samali, A., Gorman, A.M., 2016. The integrated stress response. EMBO Rep. 17 (10), 1374–1395.
Palam, L.R., Baird, T.D., Wek, R.C., 2011. Phosphorylation of eIF2 facilitates ribosomal bypass of an inhibitory upstream ORF to enhance CHOP translation. J. Biol. Chem. 286 (13), 10939–10949.
Pasini, S., Corona, C., Liu, J., Greene, L.A., Shelanski, M.L., 2015. Specific downregulation of hippocampal ATF4 reveals a necessary role in synaptic plasticity and memory. Cell Rep. 11 (2), 183–191.
Patro, R., Duggal, G., Kingsford, C., 2015. Salmon: accurate, versatile and ultrafast quantification from RNA-seq data using lightweight-alignment. BioRxiv 10, 021592.
Petrov, T., Underwood, B.D., Braun, B., Alousi, S.S., Rafols, J.A., 2001. Upregulation of iNOS expression and phosphorylation of eIF-2α are paralleled by suppression of protein synthesis in rat hypothalamus in a closed head trauma model. J. Neurotrauma 18 (8), 799–812.
Pham, M., Raymond, J., Hester, J., Kyzar, E., Gaikwad, S., Bruce, I., Fryar, C., Chanin, S., Enriquez, J., Bagawandoss, S., Zapolsky, I., Green, J., Stewart, A.M., Robison, B.D., Kalueff, A.V., 2012. Assessing Social Behavior Phenotypes in Adult Zebrafish: Shoaling, Social Preference, and Mirror Biting Tests. Zebrafish Protocols for Neurobehavioral Research. A. V. Kalueff and A. M. Stewart. Humana Press, Totowa, NJ, pp. 231–246.
Phillips, N.L., Parry, L., Mandalis, A., Lah, S., 2017. Working memory outcomes following traumatic brain injury in children: A systematic review with meta-analysis. Child Neuropsychol. 23 (1), 26–66.
Ran, Q.-S., Yu, Y.-H., Fu, X.-H., Wen, Y.-C., 2015. Activation of the Notch signaling pathway promotes neurovascular repair after traumatic brain injury. Neural Regen. Res. 10 (8), 1258–1264.
Rosarda, J.D., Giles, S., Harkins-Perry, S., Mills, E.A., Friedlander, M., Wiseman, R.L., Eade, K.T., 2023. Imbalanced unfolded protein response signaling contributes to 1-deoxysphingolipid retinal toxicity. Nat. Commun. 14 (1), 4119.
Scheper, W., Hoozemans, J.J.M., 2015. The unfolded protein response in neurodegenerative diseases: a neuropathological perspective. Acta Neuropathol. 130 (3), 315–331.
Schmidt, R., Beil, T., Strähle, U., Rastegar, S., 2014. Stab wound injury of the zebrafish adult telencephalon: a method to investigate vertebrate brain neurogenesis and regeneration. J Vis. Exper. 90 e51753.
Sidrauski, C., Acosta-Alvear, D., Khoutorsky, A., Vedantham, P., Hearn, B.R., Li, H., Gamache, K., Gallagher, C.M., Ang, K.K.H., Wilson, C., 2013. Pharmacological brake-release of mRNA translation enhances cognitive memory. eLife 2 e00498.
Sivanandam, T.M., Thakur, M.K., 2012. Traumatic brain injury: a risk factor for Alzheimer's disease. Neurosci. Biobehav. Rev. 36 (5), 1376–1381.
Soneson, C., Love, M.I., Robinson, M.D., 2015. Differential analyses for RNA-Seq: transcript-level estimates improve gene-level inferences. F1000Research 4.
Song, W., Song, Y., Kincaid, B., Bossy, B., Bossy-Wetzel, E., 2013. Mutant SOD1G93A triggers mitochondrial fragmentation in spinal cord motor neurons: neuroprotection by SIRT3 and PGC-1α. Neurobiol. Dis. 51, 72–81.
Subramanian, A., Tamayo, P., Mootha, V.K., Mukherjee, S., Ebert, B.L., Gillette, M.A., Paulovich, A., Pomeroy, S.L., Golub, T.R., Lander, E.S., 2005. Gene set enrichment analysis: a knowledge-based approach for interpreting genome-wide expression profiles. Proc. Natl. Acad. Sci. U.S.A. 102 (43), 15545–15550.
Supek, F., Bošnjak, M., Škunca, N., Šmuc, T., 2011. REVIGO summarizes and visualizes long lists of gene ontology terms. PLoS One 6 (7), e21800.
Ding, K., Gupta, P.K., Diaz-Arrastia, R., 2016. Epilepsy after traumatic brain injury. Transl. Res. Traumat. Brain Injury. Ch. 14.
Team, R. C. (2016). R: A language and environment for statistical computing. R Foundation for Statistical Computing, Vienna, Austria. http://www. R-project. org/, accessed July 2024.
Than-Trong, E., Ortica-Gatti, S., Mella, S., Nepal, C., Alunni, A., Bally-Cuif, L., 2018. Neural stem cell quiescence and stemness are molecularly distinct outputs of the Notch3 signalling cascade in the vertebrate adult brain. Development 145 (10), dev161034.
Tikhonova, M.A., Maslov, N.A., Bashirzade, A.A., Nehoroshev, E.V., Babchenko, V.Y., Chizhova, N.D., Tsibulskaya, E.O., Akopyan, A.A., Markova, E.V., Yang, Y.-L., 2022. A novel laser-based zebrafish model for studying traumatic brain injury and its molecular targets. Pharmaceutics 14 (8), 1751.

Vattem, K.M., Wek, R.C., 2004. Reinitiation involving upstream ORFs regulates ATF4 mRNA translation in mammalian cells. Proc. Natl. Acad. Sci. U.S.A. 101 (31), 11269–11274.
Walker, K.R., Tesco, G., 2013. Molecular mechanisms of cognitive dysfunction following traumatic brain injury. Front. Aging Neurosci. 5, 29.
Wang, J., Cao, H., 2021. Zebrafish and medaka: Important animal models for human neurodegenerative diseases. Int. J. Mol. Sci. 22 (19), 10766.
Wek, R.C., 2018. Role of eIF2α kinases in translational control and adaptation to cellular stress. Cold Spring Harb. Perspect. Biol. 10 (7), a032870.
Westerfield, M. (2007). The Zebrafish Book; A guide for the laboratory use of zebrafish (Danio rerio), www.zfin.org, accessed July 2024.
Wickham, H., Chang, W., Wickham, M.H., 2016. Package 'ggplot2'. Create elegant data visualisations using the grammar of graphics. Version 2 (1), 1–189.
Wu, T., Hu, E., Xu, S., Chen, M., Guo, P., Dai, Z., Feng, T., Zhou, L., Tang, W., Zhan, L., 2021. clusterProfiler 4.0: A universal enrichment tool for interpreting omics data. Innovation 2 (3), 100141.
Yu, G., Wang, L.-G., Han, Y., He, Q.-Y., 2012. clusterProfiler: an R package for comparing biological themes among gene clusters. OMICS 16 (5), 284–287.
Zhai, G., Jia, J., Bereketoglu, C., Yin, Z., Pradhan, A., 2022. Sex-specific differences in zebrafish brains. Biol. Sex Differ. 13 (1), 31.
Zhang, Z., Yan, R., Zhang, Q., Li, J., Kang, X., Wang, H., Huan, L., Zhang, L., Li, F., Yang, S., 2014. Hes1, a Notch signaling downstream target, regulates adult hippocampal neurogenesis following traumatic brain injury. Brain Res. 1583, 65–78.
Zhou, W., Y. Liang, W. Du, X. Liao, W. Fu, S. Tian, Y. Deng and X. Jiang (2023). ISRIB improves white matter injury following TBI by inhibiting NCOA4-mediated ferritinophagy. Neurochem. Intl. 177, 105744.